Available online at www.sciencedirect.com
SCIENCE DIRECT
Journal of Power Sources 128 (2004) 218–230
JOURNAL OF POWER SOURCES
www.elsevier.com/locate/jpowsour

Integration of a fuel cell into the power system using an optimal controller based on disturbance accommodation control theory

Aniruddha Paradkar [a], Asad Davari [a,*], Ali Feliachi [b], Tamal Biswas [a]

[a] Department of Electrical and Computer Engineering, West Virginia University Institute of Technology, Montgomery, WV 25136, USA
[b] Lane Department of Computer Science and Electrical Engineering, West Virginia University, Morgantown, WV 26506, USA

Received 15 September 2003; accepted 30 September 2003

Abstract

In this paper, the integration of a fuel cell into the power system is treated as a load frequency control (LFC) problem with the fuel cell acting as a load disturbance source. The integration of a fuel cell into the power system results into a change in real power. But changes in real power affect the system frequency. Thus, the integration will result into a change of frequency of the synchronous machines. Hence, we need to design a control scheme for keeping the system in the steady state. An optimal controller based on the disturbance accommodation control (DAC) theory is proposed for this load frequency control problem. For demonstrating the effectiveness of the proposed controller, we have considered a two-area power system with the fuel cell introduced in area 1. The fuel cell is considered as an external disturbance to each subsystem. A mathematical model is derived for each subsystem and based upon these models controllers are designed for keeping each subsystem stable, which in turn stabilizes the overall system. So, the proposed controller is decentralized in nature. To account for the modeling uncertainties, an observer is designed to estimate each subsystem's own and interfacing variables. The controller uses these estimates to optimize a given performance index and allocate generating unit outputs according to the requirements.

Keywords: Power system; Distributed generator; Load frequency control; Optimal control; Disturbance accommodation control; Polymer electrolyte membrane fuel cell

1. Introduction

The increasing demand for electric power forces us to consider a better economic alternative rather than increasing the load on transmission lines. The option of constructing new transmission lines is restricted because in spite of being feasible, it is not economically sound.

In order to meet the local demand, an economic alternative in the form of small generating units called distributed generators (DGs) are installed on the power system. There are different types of distributed generators and fuel cell (FC) is one of them. The integration of a fuel cell into a power system will cause a change in the real power of the system. This in turn affects the system frequency and may lead to instability in the system. Necessary control action is required to bring the system back at its normal operating condition.

In this paper, a new type of optimal controller is presented for a multi-area power system using some results from disturbance accommodation control (DAC) theory [4,5]. A power system controller is designed to integrate a polymer electrolyte membrane (PEM) fuel cell into the power system using the disturbance-utilizing mode of disturbance accommodation control. This paper proposes a load frequency control (LFC) scheme using disturbance accommodation control.

In recent years, the control of large inter-connected power systems has received an increasing attention [6,11]. It has always been of great concern to the power industry to be able to maintain electric power supply in the face of unknown system disturbance. Load frequency control or automatic generation control (AGC) is the mechanism by which energy balance is satisfied [3].

Under normal operating conditions, a power system is continually subjected to small random disturbances. Typical examples of such disturbances are small changes in the scheduled generation of one machine or a small generator such as fuel cell added to the network. Integration of fuel cell as a distributed generator to the power system can be considered as a disturbance. The transient behavior of a power system following a disturbance is in general oscillatory. If the system is stable then, these oscillations damp out towards the normal operating point. These momentary oscilla-

* Corresponding author. Tel.: +1-304-442-3205; fax: +1-304-442-3330.
E-mail address: adavari@wvu.edu (A. Davari).

0378-7753/$ – see front matter
doi:10.1016/j.jpowsour.2003.09.069

tions yield fluctuations in the power flow over transmission lines. If a certain tie line in an interconnected power system undergoes excessive power fluctuations, it may trip, thereby disconnecting the two groups of machines.

The main objectives of the research presented in this paper are:

(i) To control the frequency of synchronous machine and tie line power in each area affected due to real power of the fuel cell.
(ii) To control the power deviation of the synchronous machine in each area affected due to the online presence of the fuel cell.

This paper is organized as follows. Section 2 presents a dynamic model of the power system. An integrated model of the power system with a fuel cell is developed in Section 3. Section 4 provides some background information on the disturbance accommodation control theory. In Section 5 we design an optimal controller based upon the disturbance accommodation control theory in order to stabilize the integrated power system with the fuel cell installed. We simulate the integrated power system with the controller installed. The results obtained from the simulation are presented in Section 6. Conclusions are discussed in Section 7.

2. Dynamic model of the power system

A model of an interconnected power system consisting of a number of subsystems or control areas is given in [2]. Each area can be modeled in large details depending on the generator models and their prime movers. We introduce a fuel cell to this interconnected power system as depicted in Fig. 1.

The system is modeled as a collection of independent generation (GENCOs), transmission (TRANSCOs), and distribution (DISCOs) companies where the fuel cell is modeled as a power generator. GENCOs produce electric power that is delivered to the DISCOs either directly or through the TRANSCOs. In the structure proposed, the DISCOs are to be responsible for tracking the load and hence performing load frequency control task by securing as much transmission and generation capacity as needed. The objective of the DISCO is to supply power to its load at a nominal frequency. In case of load disturbance, GENCO 1 will adjust its output accordingly to track the load changes and maintain the energy balance.

Using the linearized dynamics of the generators, simplest models of speed governors and turbines associated with the generators, the power flow equations from generators to distribution system, and the change in load equations, the two-area test system are modeled as follows.

2.1. Dynamics of the generator

Under normal operating conditions, the relative position of the rotor axis and the resultant magnetic field axis is fixed [1,2]. The angle between the two is known as the power angle or torque angle. During any disturbance, the rotor will decelerate or accelerate with respect to the synchronously rotating air gap, and a relative motion begins.

Applying a small perturbation to the swing equation of a synchronous machine, the dynamics of the generator are given by

$$\begin{aligned}\frac{2H_1\,\mathrm{d}(\Delta f_1)}{f_0\,\mathrm{d}t} &= \Delta P_{M_1} - \Delta P_1 - D_1\,\Delta f_1\\ \frac{2H_2\,\mathrm{d}(\Delta f_2)}{f_0\,\mathrm{d}t} &= \Delta P_{M_2} - \Delta P_2 - D_2\,\Delta f_2\\ \frac{\mathrm{d}(\Delta\delta_i)}{\mathrm{d}t} &= 2\pi\,\Delta f_i\end{aligned} \quad (1)$$

where Δ represents the deviation from nominal value, H_i the constant of inertia, D_i the damping, f_0 the nominal frequency, f_i the actual frequency, δ_{I} the rotor angle, and P_{m} the turbine (mechanical) power.

2.2. Equations for speed governors and turbines

The generators are equipped with speed governors. The simplest model of a speed governor and turbine associated

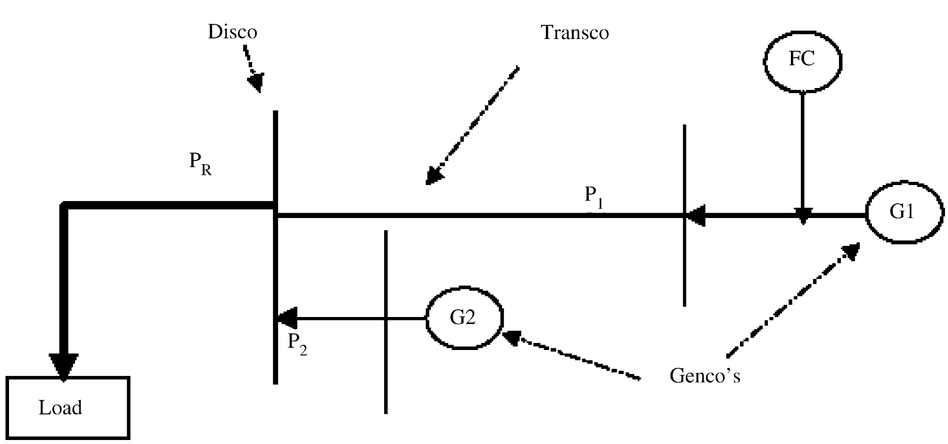

Fig. 1. Schematic diagram for integration of a fuel cell into a distribution system.

with the generator are given by

$$\frac{\mathrm{d}(\Delta P_{\mathrm{v}i})}{\mathrm{d}t} = -\frac{\Delta P_{\mathrm{v}i}}{T_{\mathrm{h}i}} + \frac{K_{\mathrm{h}i}}{T_{\mathrm{h}i}}\left(\Delta P_{\mathrm{ref}i} - \frac{\Delta f_i}{R_i}\right)$$
$$\frac{\mathrm{d}(\Delta P_{\mathrm{M}i})}{\mathrm{d}t} = -\frac{\Delta P_{\mathrm{M}i}}{T_{\mathrm{M}i}} + \frac{K_{\mathrm{M}i}}{T_{\mathrm{M}i}}\Delta P_{\mathrm{v}i} \quad (2)$$

where P_{v} is the steam valve power, T_{m} and T_{h} the time constants of turbine and governor, K_{m} and K_{h} the gain constants of turbine and governor, R_i the droop characteristics, and $P_{\mathrm{ref}i}$ the reference set-point.

2.3. Power angle equations

The relation between rotor dynamics and the swing equation is expressed by [2] as

$$\frac{2H}{\omega_{\mathrm{s}}}\frac{\mathrm{d}^2\delta}{\mathrm{d}t^2} = P_{\mathrm{a}} = P_{\mathrm{m}} - P_{\mathrm{e}} \quad (3)$$

In the swing Eq. (3) for the generator, the input mechanical power from the prime mover, P_{m}, will be considered constant. This is a reasonable assumption because conditions in the electrical network can be expected to change before the control governor can cause the turbine to react. Since P_{m} is constant, the electrical power output P_{e} will determine whether the rotor accelerates, decelerates, or remains at synchronous speed. When P_{e} equals P_{m}, the machine operates at steady-state synchronous speed; when P_{e} changes from this value, the rotor deviates from synchronous speed. Conditions on the transmission and distribution networks and the loads on the system to which the generator supplies power determine changes in P_{e}. Electrical network disturbances resulting from severe load changes, network faults, or circuit-breaker operations may cause the generator output P_{e} to change rapidly.

Our fundamental assumption in this work is that the effect of machine speed variations upon the generated voltage is negligible so that the manner in which P_{e} changes are determined by the power-flow equations applicable to the state of the electrical network and by the model chosen to represent the electrical behavior of the machine. Each synchronous machine is represented for transient stability studies by its transient internal voltage V_i in series with the transient reactance X_i, V_{t} is the terminal voltage. This corresponds to the steady-state representation in which synchronous reactance X is in series with the internal or no-load voltage V_i.

Let P and Q represent real and reactive power of the system.

We have,

$$P_k + jQ_k = V_K\sum_{n=1}^{N}(Y_{kn}V_n)\angle\phi i_n + \Delta\delta_n - \Delta\delta_i \quad (4)$$

Let us assume the initial condition as $k = 1$ and $N = 2$. Therefore, we have

$$P_1 + jQ_1 = V_1(Y_{11}V_1)^* + V_1(Y_{12}V_2)^*$$

We define

$$V_1 = |V_1|\angle\Delta\delta_1$$
$$V_2 = |V_2|\angle\Delta\delta_2$$
$$Y_{11} = G_{11} + jB_{11}$$
$$Y_{12} = |Y_{12}|\angle\phi_{12} \quad (5)$$

The above equation yields

$$P_1 = |V_1|^2G_{11} + |V_1||V_2||Y_{12}|\cos(\Delta\partial_1 - \Delta\partial_2 - \phi_{12})$$
$$Q_1 = |V_1|^2B_{11} + |V_1||V_2||Y_{12}|\sin(\Delta\partial_1 - \Delta\partial_2 - \phi_{12}) \quad (6)$$

We assume

$$\Delta\delta = \Delta\delta_1 - \Delta\delta_2 \quad (7)$$

and define a new angle γ such that

$$\gamma = \phi_{12} - \frac{\pi}{2}$$

The above equation then changes to

$$\Delta P_{\mathrm{e}} = \Delta P_{\mathrm{c}} + \Delta P_{\max}\sin(\delta - \gamma) \quad (8)$$

The above equation is often called as the power angle equation. The parameters P_{c}, $P_{\max}$, and γ are constants for a given network configuration and constant voltage magnitudes $|V_1|$, $|V_2|$. When the network is considered without resistance all the elements of Y_{bus} are susceptances, and therefore G_{11} and γ are zero. Then, the power angle equation becomes

$$\Delta P_1 = T_1\sin(\Delta\delta_1 - \Delta\delta_3)$$
$$T_1 = \frac{|V_1|\,|V_3|\,\cos(\delta_1^0 - \delta_3^0)}{X_1} = P_{\max} \quad (9)$$

This is indeed the familiar equation, which applies for pure reactance network given by

$$\Delta P_{\mathrm{e}} = P_{\max}\sin(\delta) \quad (10)$$

where

$$P_{\max} = \frac{|V_i||V_2|\cos(\delta)}{X_i}$$

Similarly, when we apply the power angle equation to bus 2, we get

$$\Delta P_2 = T_2\sin(\Delta\delta_2 - \Delta\delta_3) \quad (11)$$

where

$$T_2 = \frac{|V_2|\,|V_3|\,\cos(\delta_2^0 - \delta_3^0)}{X_2}$$

The following properties hold in a well designed and properly operated power system:

(i) The angular differences $(\delta_1 - \delta_2)$ between typical buses are so small that

$$\cos(\delta_i - \delta_j) = 1;$$
$$\sin(\delta_i - \delta_j) = (\delta_i - \delta_j)$$

(ii) The line susceptances B_{ij} are many times larger than the line conductance G_{ij} so that

$$G_{ij}\sin(\delta_i-\delta_j) \ll B_{ij}\cos(\delta_i-\delta_j)$$

(iii) The reactive power Q_i injected into any bus I of the system during normal operation is much less than the reactive power which would flow if all lines from that bus were short circuited to reference, i.e. $Q_i \lll |V_i|^2 B_{ij}$.

Therefore, power flows between GENCO and DISCO are given by

$$\begin{aligned}\Delta P_1 &= T_1(\Delta\delta_1-\Delta\delta_3)\\ \Delta P_2 &= T_2(\Delta\delta_2-\Delta\delta_3)\\ \Delta P_2 &= -T_2(\Delta\delta_1-\Delta\delta_2)+T_2(\Delta\delta_1-\Delta\delta_3)\end{aligned} \tag{12}$$

where

$$T_i=\frac{|V_i|\,|V_3|}{X_i}=P_{\max}$$

The change in load is expressed by

$$\begin{aligned}\Delta P_L &= \Delta P_1+\Delta P_2=(T_1+T_2)(\Delta\delta_1-\Delta\delta_3)\\ &\qquad -T_2(\Delta\delta_1-\Delta\delta_2)\\ (\Delta\delta_1-\Delta\delta_3) &= \frac{\Delta P_L}{T_1+T_2}+\frac{T_2}{T_1+T_2}(\Delta\delta_1-\Delta\delta_2)\end{aligned} \tag{13}$$

2.4. Model for the power system

The state space model of the power system as derived from the above equations is given by

$$\begin{aligned}\dot{x} &= Ax+Bu+Gw\\ x^{\mathrm{T}} &= [\Delta f_1 \quad \Delta P_{M_1} \quad \Delta P_{V_1} \quad \Delta\delta_1-\Delta\delta_2 \quad \Delta f_2 \quad \Delta P_{M_2} \quad \Delta P_{V_2}]\\ u &= \Delta P_{\mathrm{ref}1}\\ w^{\mathrm{T}} &= [\Delta P_L]\end{aligned} \tag{14}$$

where

$$A=\begin{bmatrix} \frac{-D}{T_{P_1}} & \frac{1}{T_{P_1}} & 0 & \frac{-\alpha}{T_{P_1}} & 0 & 0 & 0\\ 0 & -\frac{1}{T_{M_1}} & \frac{K_{M_1}}{T_{M_1}} & 0 & 0 & 0 & 0\\ \frac{-K_{H_1}}{R_1T_{H_1}} & 0 & -\frac{1}{T_{H_1}} & 0 & 0 & 0 & 0\\ 2\pi & 0 & 0 & 0 & -2\pi & 0 & 0\\ 0 & 0 & 0 & \frac{-\alpha}{T_{P_2}} & \frac{-D_2}{T_{P_2}} & \frac{1}{T_{P_2}} & 0\\ 0 & 0 & 0 & 0 & 0 & -\frac{1}{T_{M_2}} & \frac{K_{M_2}}{T_{M_2}}\\ 0 & 0 & 0 & 0 & \frac{-K_{H_2}}{R_2T_{H_2}} & 0 & -\frac{1}{T_{H_2}} \end{bmatrix}$$

$$\alpha=\frac{T_1T_2}{T_1+T_2}$$

$$T_{P_i}=\frac{2H_i}{f_0}$$

$$B^{\mathrm{T}}=\begin{bmatrix}0 & 0 & \frac{K_{H_1}}{T_{H_1}} & 0 & 0 & 0 & \frac{K_{H_2}}{T_{H_2}}\end{bmatrix}$$

$$G^{\mathrm{T}}=\begin{bmatrix}\frac{-T_1}{(T_1+T_2)T_{P_1}} & 0 & 0 & 0 & \frac{-T_2}{(T_1+T_2)T_{P_1}} & 0 & 0\end{bmatrix}$$

3. Integrated model of power system with fuel cell

In Section 2.4, we derived a state variable model for the power system. This model can be represented in the generalized form as

$$\begin{aligned}\dot{x} &= f(x,u,t)\\ y &= z(x,u)\end{aligned} \tag{15}$$

After the integration of the fuel cell into the power system, we can remodel the overall system as

$$\begin{aligned}\dot{x} &= f(x+x_{\mathrm{F}},u,t)\\ y &= z(x+x_{\mathrm{F}},u)\end{aligned} \tag{16}$$

where x_{F} is a new variable introduced as a result of the integration of the fuel cell.

We have chosen a PEM fuel cell for its easy and safe operational modes, low-temperature gradient, less chance of catalyst poisoning and a wide scope of application in power distribution system [8–10]. A detailed modeling and simulation of the dynamic behavior of this fuel cell has been carried out in [10].

The result of the chemical reactions inside a fuel cell is the reversible single electrode potential, E_r given by the Nernst equation as

$$E_r = E_r^o - \left[\left(\frac{RT}{nF}\right)\ln\left(\frac{p_{H_2O}}{p_{H_2}\times\sqrt{p_{O_2}}}\right)\right] \quad (17)$$

where E_r^o is the standard electrode potential, R the gas constant (8.3144 J/mol K), T the temperature in Kelvin scale, n the number of electrons per reacting ion or molecule, F represents Faraday's constant (96,500 C/mol), p_{H_2O} the partial pressure of water, p_{H_2} the partial pressure of hydrogen, and p_{O_2} the partial pressure of oxygen.

A chemical polarization of cell voltage takes place due to the individual chemical reactions occurring at the electrodes of the fuel cell. This is given by the Tafel equation as

$$\Delta E_{Chem} = \left[\frac{RT}{\alpha nF}\right]\ln i_o + 2.303\left[\frac{RT}{\alpha nF}\right]\log(I) \quad (18)$$

where α is the activity coefficient, i_o the exchange current density, and I the applied current density.

There is a change in the concentration gradient at the electrodes due to the continuous chemical reactions. The effects of these changes are expressed in the form of concentration polarization as follows:

$$\Delta E_{Conc} = \left[\frac{RT}{nF}\right]\ln\left(\frac{I_L - I}{I_L}\right) \quad (19)$$

where I_L is the limiting current density and I the applied current density.

As a result of the electrochemical reactions, there is a certain amount of change in specific conductivity, leading to an additional loss in the potential given by

$$\Delta E_{Rest} = \frac{nFD}{\Lambda(1-t_i)}\ln\left(\frac{I_L - I}{I_L}\right) \quad (20)$$

where Λ represents the equivalent conductance of the reacting ion (cm^2/ohm-equiv), t_i the transference number, and D the diffusion constant.

So, the sum total of all pertinent components of polarization (ΔE_T) occurring in a single cell is given by

$$\Delta E_T = \Delta E_{Chem} + \Delta E_{Conc} + \Delta E_{Rest} \quad (21)$$

Thus, for a closed circuit cell with voltage V, operating at a load current i, the voltage is expressed as follows:

$$V = (E_{r,A} - \Delta E_{T,A}) - (E_{r,C} - \Delta E_{T,C}) - i\sum R_j$$

$$V = E_{T,r} - \Delta E_{T,A} + \Delta E_{T,C} - i\sum R_j \quad (23)$$

where $E_{T,r}$ is combined standard electrode potential of anode and cathode, $\Delta E_{T,A}$ the sum total of all pertinent components of anodic polarization (a positive number), and $\Delta E_{T,C}$ the sum total of all pertinent components of cathode polarization (a negative number), 'i' the total current through the cell, and $\sum R_j$ represents the sum of all internal cell resistance including electrolyte, any diaphragms, and resistances in the electrode bodies.

The total power output from the fuel cell is given as

$$P_{1\,cell} = V_o I_o \quad (24)$$

where V_o is the output voltage of a single-phase inverter and I_o the output current.

Using the voltage dynamics of a single-phase bridge inverter as well as the stack current dynamics of the fuel cell, we get

$$\begin{aligned}\dot{P}_{1\,cell} = {} & \frac{V_r - \Delta E_T}{nRT}\left(\frac{n_i F\Delta P_T(t)}{dt}\right)P_{1\,chem} \\ & + \left(\frac{\Delta P_T(t)}{dt} - \frac{RT_s}{V_s}(m_i X_i - m_0 X_i)\right) \\ & \times \frac{V_s(n_i F)\cos\alpha}{nRT_s}\left(\frac{I_0}{I}\frac{RT}{\alpha nF}\ln\left(\frac{I}{I_0}\right) + A + B\right)\end{aligned} \quad (25)$$

where

$$A = \frac{p_0}{p_a}\frac{RT}{nF}\ln\left(\frac{p_a}{p_0}\right)$$

$$B = \frac{I_L}{I_L - I}\frac{nFD}{\Delta(1-t_i)}\ln\left(\frac{I_L - I}{I_L}\right)$$

Although the appearance of the fuel cell is only restricted to area 1, there may be a possibility that the effects of control actions and/or the fuel cell itself may have some impact on area 2 through interconnections. These are taken into consideration while developing a model for the integrated power system. We develop a model for the fuel cell with the states being Δf_{FC}, $\Delta P_{1\,chem}$, $\Delta P_{1\,cell}$, $\Delta P_{tie\text{-}FC}$, z_1, z_2, z_3. It is very important to note that z_1, z_2, z_3 denote the impact of the fuel cell on area 2.

The state space model of the fuel cell is given as follows [10]:

$$\begin{aligned}\dot{x}_F &= A_F x_F + B_F u \\ w &= C_F x_F\end{aligned} \quad (26)$$

where

$$x_F^T = [\,\Delta f_F \quad \Delta P_{1\,cell} \quad \Delta P_{1\,chem} \quad \Delta P_{tie-F} \quad z_1 \quad z_2 \quad z_3\,]$$

$$A_F = \begin{bmatrix} 0 & 0 & 0 & 0 & 0 & 0 & 0 \\ 0 & 0 & \dfrac{-n\overline{h}(V-\Delta E_T)\Delta H}{T} & 0 & 0 & 0 & 0 \\ 0 & 0 & \dfrac{V-\Delta E_T}{NRT}\left(\dfrac{n_i F\Delta\Delta_T(t)}{dt}\right) & 0 & 0 & 0 & 0 \\ 0 & 0 & 0 & 0 & 0 & 0 & 0 \\ 0 & 0 & 0 & 0 & 0 & 1 & 0 \\ 0 & 0 & 0 & 0 & 0 & 0 & 1 \\ 0 & 0 & 0 & 0 & 0 & 0 & 0 \end{bmatrix};$$

$$B_{\mathrm{F}} = \begin{bmatrix} 0 \\ 0 \\ \left(\dfrac{\Delta P_{\mathrm{T}}(t)}{\mathrm{d}t} - \dfrac{RT_{\mathrm{s}}}{(V-\Delta E_{\mathrm{T}})}(m_i X_i - m_0 X_i)\right) \dfrac{(V-\Delta E_{\mathrm{T}})(n_i F)\cos\alpha}{nRT_{\mathrm{s}}} \left(\dfrac{I_0}{I}\dfrac{RT}{\alpha nF}\ln\left(\dfrac{I}{I_0}\right) + A + B\right) \\ 0 \\ 0 \\ 0 \\ 0 \end{bmatrix}$$

$$B = \frac{p_0}{p_{\mathrm{a}}}\frac{RT}{nF}\ln\left(\frac{p_{\mathrm{a}}}{p_0}\right)$$

$$A = \frac{I_{\mathrm{L}}}{I_{\mathrm{L}} - I}\frac{nFD}{\Delta(1-t_i)}\ln\left(\frac{I_{\mathrm{L}} - I}{I_{\mathrm{L}}}\right)$$

3.1. Linear model for the fuel cell

The above model of the fuel cell is nonlinear and cannot be used directly for controller design or transient stability analysis. We need a linear model for the fuel cell system. After making some assumptions based on practical data we transform the nonlinear model of the fuel cell into a linear one given as

$$\begin{aligned} \dot{x}_{\mathrm{F}} &= A_{\mathrm{F}} x_{\mathrm{F}} + B_{\mathrm{F}} u \\ w &= C_{\mathrm{F}} x_{\mathrm{F}} \end{aligned} \qquad (27)$$

where

$$x_{\mathrm{F}}^{\mathrm{T}} = \begin{bmatrix} \Delta f_{\mathrm{F}} & \Delta P_{1\,\mathrm{cell}} & \Delta P_{1\,\mathrm{chem}} & \Delta P_{\text{tie-F}} & z_1 & z_2 & z_3 \end{bmatrix}$$

$$A_{\mathrm{F}} = \begin{bmatrix} 0 & 0 & 0 & 0 & 0 & 0 & 0 \\ 0 & 0 & 1 & 0 & 0 & 0 & 0 \\ 0 & 0 & -0.25 & 0 & 0 & 0 & 0 \\ 0 & 0 & 0 & 0 & 0 & 0 & 0 \\ 0 & 0 & 0 & 0 & 0 & 1 & 0 \\ 0 & 0 & 0 & 0 & 0 & 0 & 1 \\ 0 & 0 & 0 & 0 & 0 & 0 & 0 \end{bmatrix};$$

$$B_{\mathrm{F}} = \begin{bmatrix} 0 \\ 0 \\ 1 \\ 0 \\ 0 \\ 0 \\ 0 \end{bmatrix}; \quad C_{\mathrm{F}}^{\mathrm{T}} = \begin{bmatrix} 0 \\ 101 \\ -2843 \\ 0 \\ 1 \\ 0 \\ 0 \end{bmatrix}$$

3.2. Integrated system model

Using relations (14) and (27), we derive a state space model of the power system with the fuel cell integrated in it. This state space model is given as

$$\dot{x}_i = \begin{bmatrix} A & I \\ 0 & A_{\mathrm{F}} \end{bmatrix} x_i + \begin{bmatrix} B \\ B_{\mathrm{F}} \end{bmatrix} u + \begin{bmatrix} G \\ 0 \end{bmatrix} w \qquad (28)$$

$$\dot{x}_i = A_I x_i + B_I u + G_I w \qquad (29)$$

A_{I} and B_{I} represent the integrated power system model, A and B the original power system model, and A_{F} and B_{F} the fuel cell model and its impacts on the neighboring subsystem.

The model represented by Eq. (29) will be used for designing an optimal controller for a smooth integration of the fuel cell.

4. Disturbance accommodation control theory

Design of optimal controllers based upon DAC theory began in 1967 [4,5] and has since been developed and refined to the point where it is now a practical and general-purpose design tool ideally suited for industrial control applications.

Power system disturbances are not totally erratic, but have a waveform structure, that is they can be mathematically modeled as a weighted linear combination of a set of known basis functions given as

$$x_{\mathrm{F}}(t) = C_1 f_1(t) + C_2 f_2(t) + C_3 f_3(t) + \cdots \qquad (30)$$

where the basis functions $f_i(t)$ represent the various waveform patterns.

If we can represent the unknown input disturbance $x_{\mathrm{F}}(t)$ by waveform mode characterization, it is possible to disregard all statistical considerations, random process theories etc. and proceed to design a physically realizable deterministic type of feedback controller based upon DAC theory. These types of controllers are remarkably effective in coping with the specified class of disturbance. In fact, when the disturbances $x_{\mathrm{F}}(t)$ have waveform structure, DAC typically yields significantly better performance than the so called stochastic controllers which are designed by considering only the experimentally measured long term statistical properties of $x_{\mathrm{F}}(t)$ [5].

In the field of applied control technology, it is a well-known fact that all realistic control systems operate in environments that produce system disturbances of one kind or another. Here, the term disturbance refers to those specific categories of the system inputs that are not accurately known beforehand and which, cannot be manipulated by the control designer i.e. uncontrollable inputs. Disturbances are an important factor in control design because they introduce unwanted disruptions to the otherwise orderly behavior of the controlled system. A good control system should be designed in such a way that it maintains the given control specifications in the face of all disturbances that might act on the system under actual operating conditions.

The disturbance accommodation control theory allows us to systematically design multivariable feedback control systems that are remarkably effective in coping with both transient and persistent disturbances encountered in large power systems.

There can be different types of disturbance accommodation controller [4].

They are:

(1) absorption type,
(2) minimization type, and
(3) utilization type.

In this paper, we will be considering the utilization type disturbance accommodation controller.

5. Control of power distribution system using the utilization mode of DAC theory

The main idea behind the working of a disturbance accommodation controller in its utilization mode is that disturbances might sometimes be capable of producing desirable effects on the system behavior. From a conservative point of view we can say that some of the disturbances can be constructively used as an aid in carrying out the primary control objective. For example, the control energy and/or the transition time required to bring the system states $x(t)$ to some given set point x_{sp} might be reduced if we take advantage of the natural perturbed motion of $x(t)$ caused by the action of disturbances. Of course, we have to manipulate the control $u(t)$ so as to harness and exploit the useful effects in the disturbances.

If the disturbance $x_F(t)$ has a waveform structure that can be modeled, we can employ optimal control theory to design a disturbance accommodating controller that makes optimal utilization of the disturbances [4].

5.1. Integration of fuel cell into power distribution system using disturbance accommodating controller

An optimal controller is designed to achieve the smooth integration of a fuel cell into the power distribution system. Here, maximum utilization of the fuel cell output $x_F(t)$ takes place. We regulate the system frequency deviation Δf_1 and Δf_2 to zero while keeping the time interval of frequency deviation as small as possible.

The primary control objective is to regulate the system output $y(t) = C(t)x(t)$ from any initial condition $y(t_o) = C(t_o)x(t_o)$ to the given set point $y(T) = y_{sp}$ where the termination time T is a fixed priori. To achieve this primary control objective and simultaneously make maximum utilization of the fuel cell output $x_F(t)$, we choose the control $u(t)$ to minimize the quadratic performance criterion given by [4,5]

$$J = \frac{1}{2}e'(t)\,Se(t) + \frac{1}{2}\int_{t_o}^{T}[e'(t)\,Qe(t) + u'(t)\,Ru(t)]\,dt \tag{31}$$

where S, $Q(t)$, and $R(t)$ are positive definite symmetric weighting matrices chosen by the designer, $e(t)$ denotes the set point error $e(t) = y_{sp} - y(t)$ and $[t_o\ T]$ is the specified time interval.

Now, we introduce the augmented state vector $\tilde{x} = [\,x \quad y_{sp} \quad x_F\,]^T$. So, the composite set with the condition $\dot{y}_{sp} = 0$ can be written as

$$\dot{\tilde{x}} = \begin{bmatrix} A & 0 & GC_F \\ 0 & 0 & 0 \\ 0 & 0 & A_F \end{bmatrix}\begin{pmatrix} x \\ y_{sp} \\ x_F \end{pmatrix} + \begin{bmatrix} B \\ 0 \\ 0 \end{bmatrix} u \tag{32}$$

The set point error e can be expressed in terms of $\tilde{x}$ as

$$e = \begin{bmatrix} -C & I & 0 \end{bmatrix}\tilde{x} \tag{33}$$

The linear quadratic optimal control theory is applied to determine the control, which minimizes (31). The final expression for the disturbance accommodating controller is

$$u(x, x_F, y_{sp}, t) = -(R^{-1}B'K_x)'x - (R^{-1}B'K_y)y_{sp} - (R^{-1}B'K_x)x_F \tag{34}$$

where K_x, K_y, K_z are time varying matrices to be computed off line by numerical solution of the set of matrix differential equations given as

$$\begin{aligned} \dot{K}_x &= (-A + BR^{-1}B'K_x)'K_x - K_xA - C'QC; \qquad K_x(T) = C'SC \\ \dot{K}_y &= (-A + BR^{-1}B'K_x)'K_y + C'Q; \qquad K_y(T) = -C'S \\ \dot{K}_z &= (-A + BR^{-1}B'K_x)'K_z - K_zA_F - K_xC_F; \qquad K_z(T) = 0 \end{aligned} \tag{35}$$

A part of the control signal is governed by the Area Control Error which is generated by the system during load changes. This is represented by the term $-(R^{-1}B'K_x)'x$. Also part of the control signal is governed by the fuel cell output since we feedback the fuel cell output. This is represented by the term $-(R^{-1}B'K_x)x_F$. The term $-(R^{-1}B'K_y)y_{sp}$ governs the set point associated with the system.

Solving Eqs. (34) and (35) yields [7],

$$u(x, x_F, y_{sp}, t) = \begin{bmatrix} -495.94 & -166.82 & -10.59 & -253.21 & 126.21 & 28.95 & 1.16 \end{bmatrix} y + \begin{bmatrix} 0 & -101 & 2843 & 0 & 0 & -10 & 0 \end{bmatrix} x_F - 243\, y_{sp} \quad (36)$$

The variables x and x_F cannot be measured directly from the system. So for the purpose of implementation we replace x and x_F by $\hat{x}$ and $\hat{x}_F$, which are the outputs of an observer.

5.2. Observer design

A large-scale power system consists of in general, a number of interconnected subsystems. Although interconnection is necessary for the economical operation of the overall system, there is a possibility that control actions and/or external disturbances occurring in one subsystem will be transmitted via the interconnections to the neighboring systems and thereby producing undesirable effects. Hence, in an interconnected power system, not all the state variables are measurable, and the interface variables cannot be obtained from local measurements. An observer is used to overcome this limitation by estimating the required state and interface variables using only available measurements.

The output of the observer $\hat{x}$ and $\hat{x}_F$ are obtained from

$$\begin{bmatrix} \dot{\hat{x}} \\ \dot{\hat{x}}_F \end{bmatrix} = \begin{bmatrix} A + K_1 C & FC_F \\ K_2 C & A_F \end{bmatrix} \begin{bmatrix} \hat{x} \\ \hat{x}_F \end{bmatrix} + \begin{bmatrix} B \\ 0 \end{bmatrix} u(t) - \begin{bmatrix} K_1 \\ K_2 \end{bmatrix} y(t) \quad (37)$$

where u and y are, respectively, the actual output and the control input of the original plant, and K_1, K_2 the gain matrices.

These gain matrices K_1 and K_2 are designed by examining the error dynamics associated with the observer. We define

$$\epsilon_x = x - \hat{x}$$
$$\epsilon_y = y - \hat{y} \quad (38)$$

Then, the error dynamics are given as

$$\begin{bmatrix} \epsilon_x \\ \epsilon_y \end{bmatrix} = \begin{bmatrix} A + K_1 C & FC_F \\ K_2 C & D \end{bmatrix} \begin{bmatrix} \epsilon_x \\ \epsilon_y \end{bmatrix} \quad (39)$$

where K_1 and K_2 are chosen so in such a way that the transient solution of the above equation will approach zero.

Applying linear observer design techniques along with pole placement methodology to the above equations, the following gain matrices are obtained

$$K_1^T = \begin{bmatrix} -57610; & 6060; & -58000; & -155220; & -53710; & 9830; & 10580 \end{bmatrix}$$
$$K_2^T = \begin{bmatrix} -160; & 30; & -10; & -181600; & -28210; & -2390; & -100 \end{bmatrix} \quad (40)$$

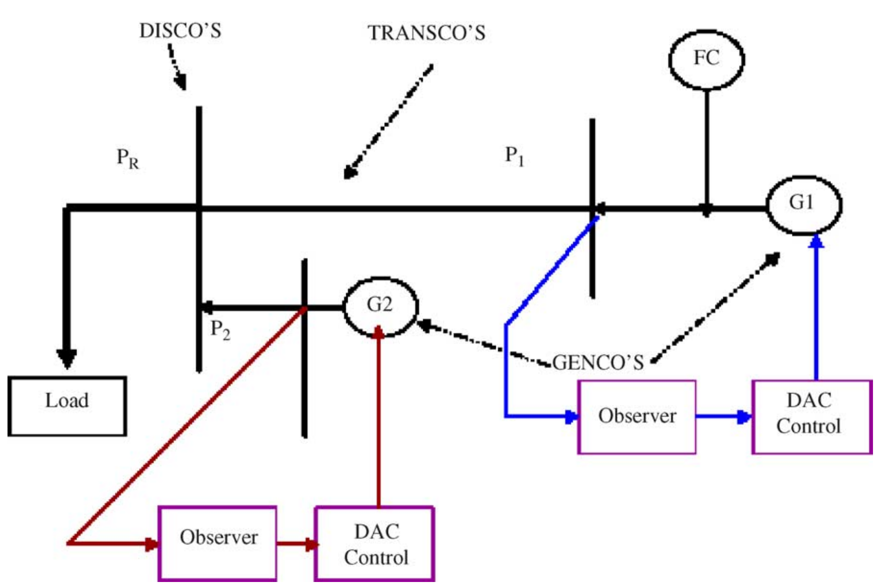

Fig. 2. Integrated power system with the controller installed.

A schematic diagram of the integrated system with the controller installed is shown in Fig. 2. It depicts a two-area distribution system undergoing load frequency control. G1 and G2 are the synchronous machines (generators) of two different areas. The fuel cell is connected in area 1. The difference between the proposed scheme and conventional load frequency control is that instead of feeding back the tie line power and frequency deviation we will be feeding back the tie line power, frequency deviation, and the fuel cell output back to the generators [7]. The results of this innovative scheme are presented in Section 6.

The main functions of the proposed controller are as follows:

(1) To keep the system frequency approximately at the nominal value (60 Hz).
(2) To maintain the tie-line power flow at scheduled value.
(3) To regulate the generator outputs such that each area absorbs its own load changes.

In the next section, the simulation results are given to show how well the controller achieves these objectives.

6. Simulation results

6.1. Tracking performance of the integrated power system for different types of load

Figs. 3 and 4 represent the simulation results of the power system incorporating fuel cell and a tracking load. Fig. 3 represents the tracking of the system to a sine load where as Fig. 4 represents the tracking of the system to a square load. The output of the system is tracking the input very well except for the overshoot at the start.

6.2. Power deviation and frequency deviation using a disturbance accommodating controller

When the fuel cell is connected to the power system, there will be some oscillations in the output of the generators which should be dampened out quickly to avoid any damage to the appliances connected to the system. Ideally, the power flow through the tie line is zero. But during a disturbance power starts flowing through the tie line. This flow of power gradually becomes zero as the system becomes stable. Similarly, during normal conditions the power system operates at a particular frequency. But at the time of a disturbance some deviation from this normal frequency takes place.

Fig. 5 represents the power deviation and the tie line power flow when the fuel cell is incorporated into the power system and there is no controller installed.

From the above response, one can see that the system oscillates rapidly when the fuel cell is added to the system and takes about 100 s to become stable. So, we incorporate a disturbance accommodating controller to bring the system back to its normal condition as soon as possible.

Fig. 6 represents the power deviation and the tie line power flow when the disturbance accommodating controller is present. The system takes about 7 s to become stable.

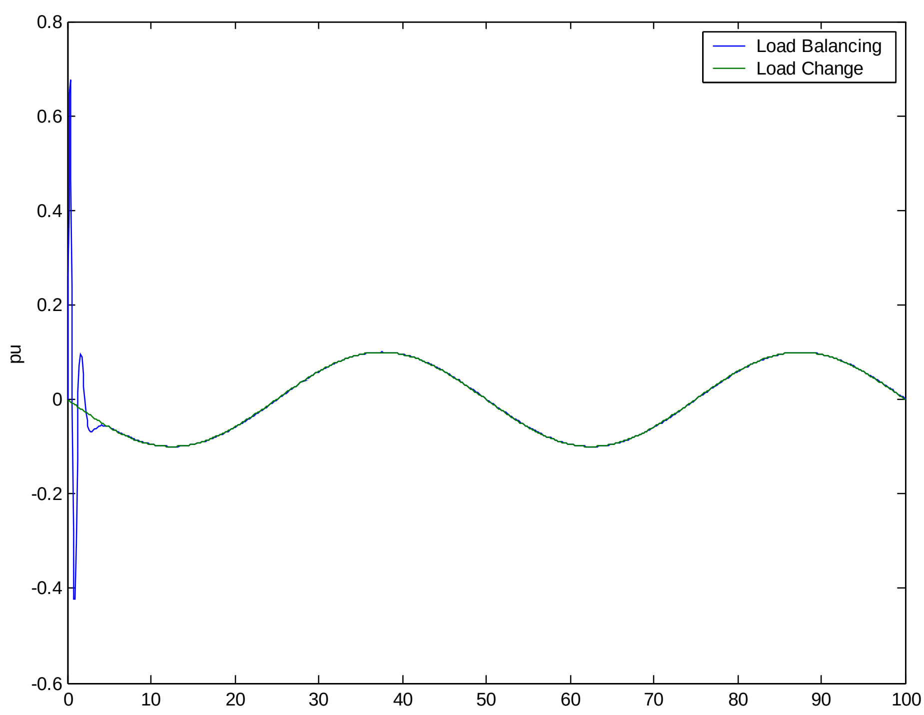

Fig. 3. Tracking behavior of the integrated power system for a sinusoidal load.

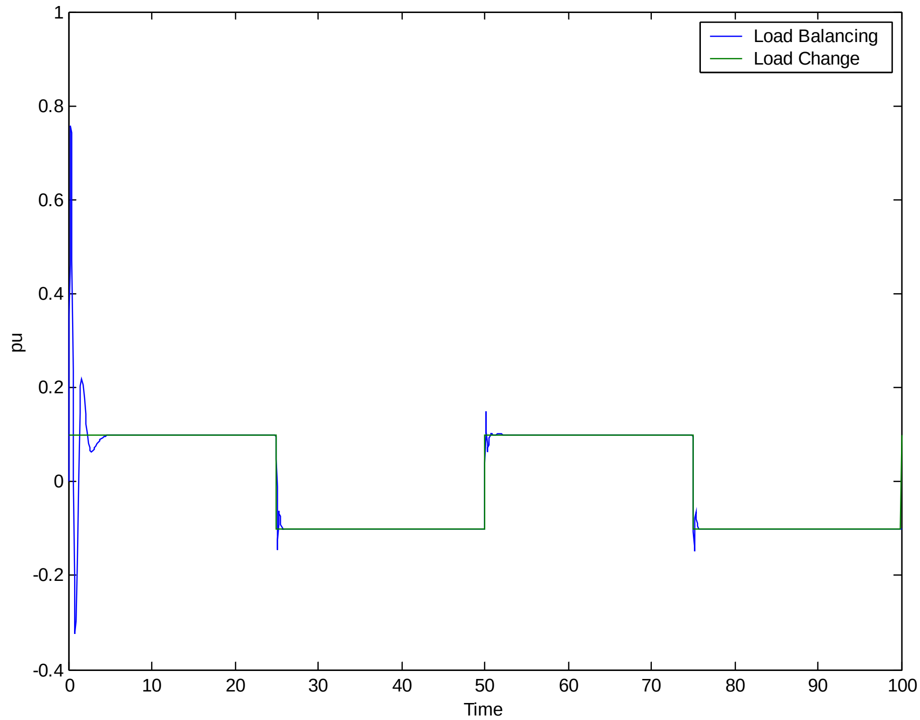

Fig. 4. Tracking behavior of the integrated power system for a square load.

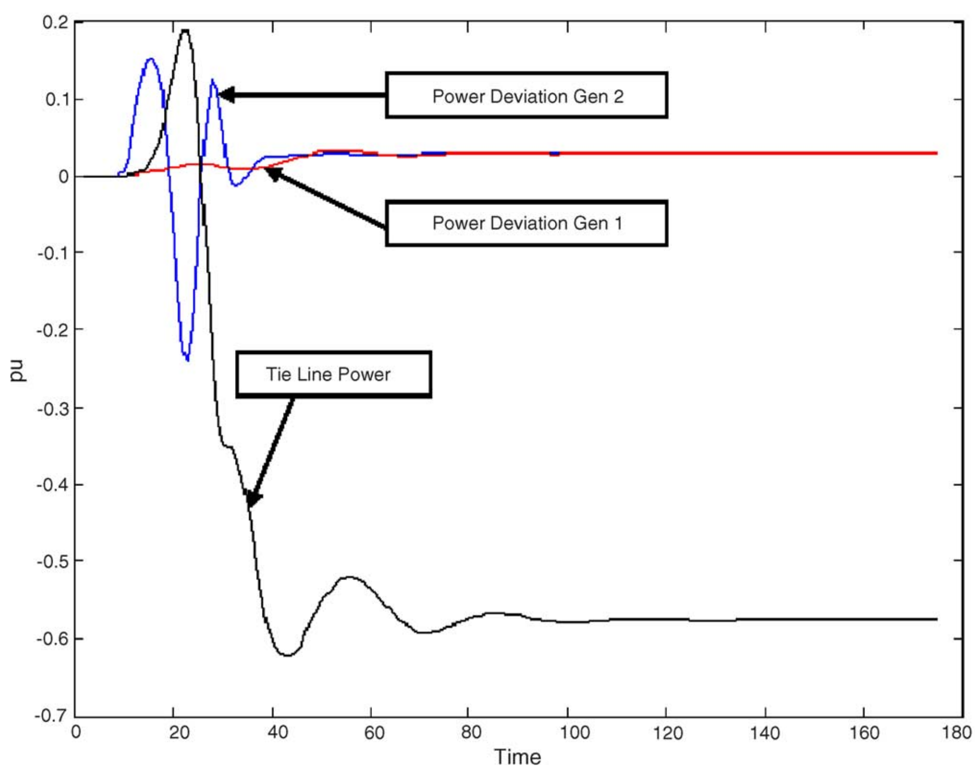

Fig. 5. Power deviation and tie line power flow without the disturbance accommodating controller.

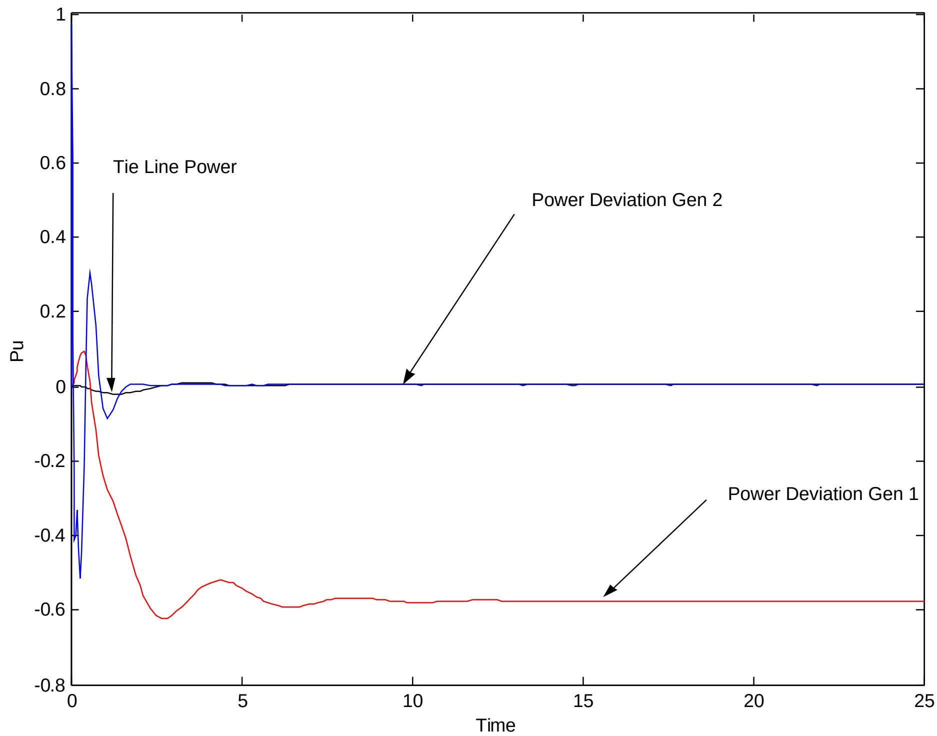

Fig. 6. Power deviation and tie line power flow with the disturbance accommodating controller installed.

So we see that the system returns to its normal operating condition much faster than the previous case when the controller was not installed. This implies that the disturbance accommodating controller is very effective in controlling the system.

Fig. 7 represents the frequency deviation when the fuel cell is incorporated into the power distribution system without any controller. As real power from the fuel cell is added to the system, the system frequency gradually increases and the system becomes unstable.

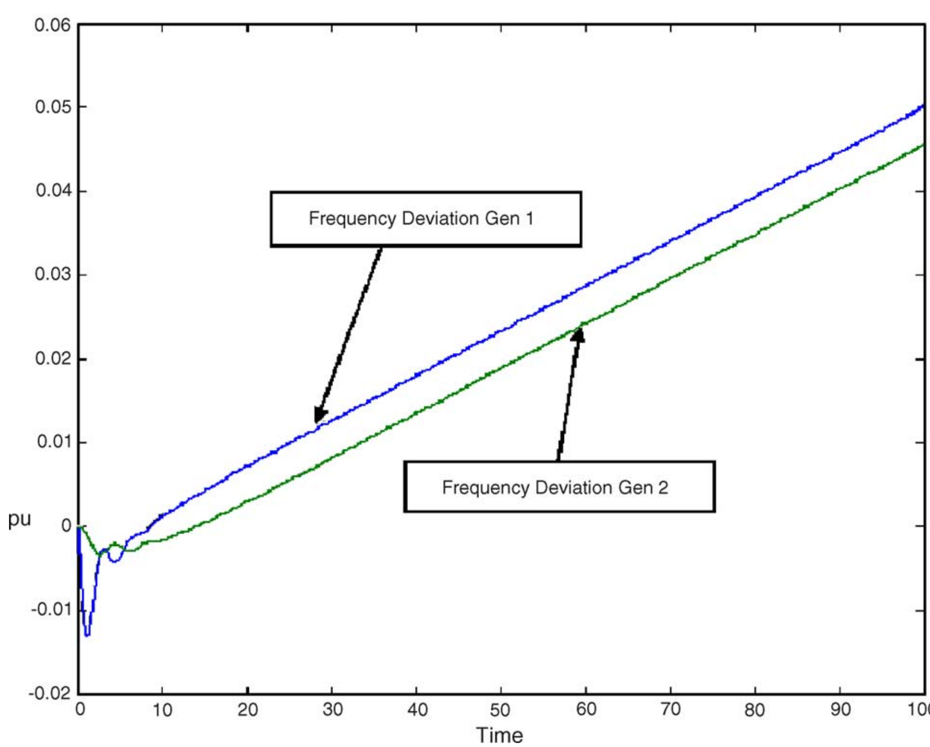

Fig. 7. Frequency deviation without the disturbance accommodating controller.

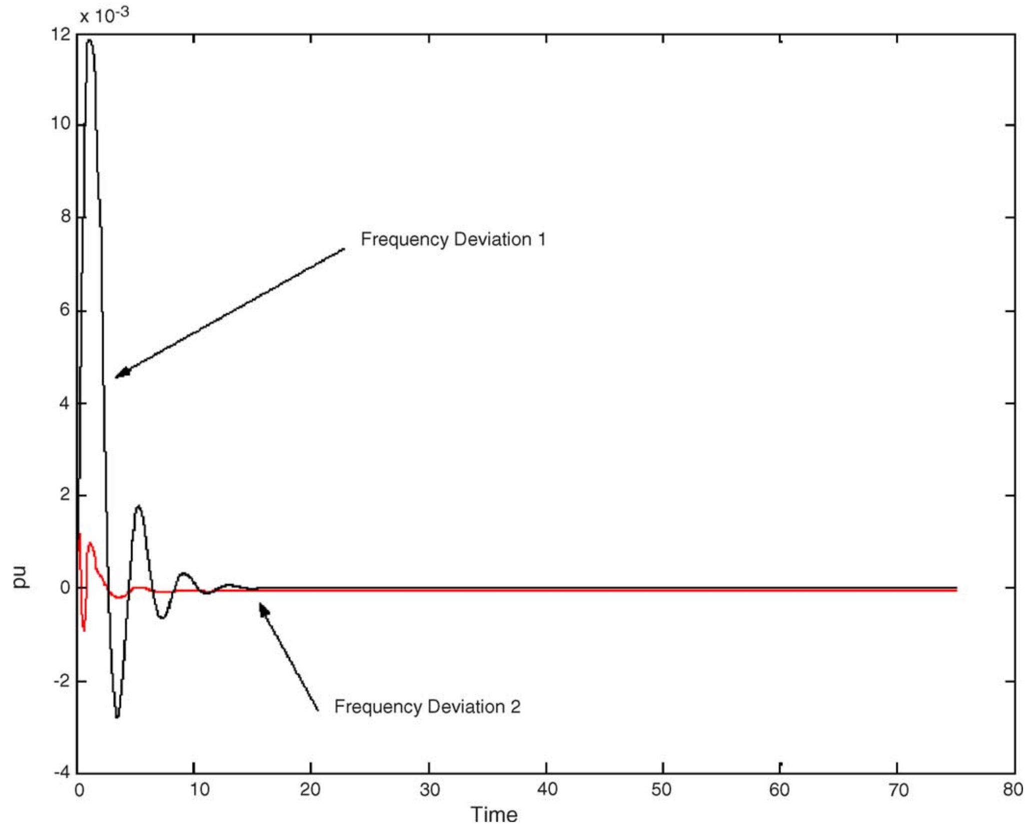

Fig. 8. Frequency deviation with the disturbance accommodating controller installed.

Fig. 8 represents the frequency deviation when the fuel cell is integrated into the power distribution system in the presence of a disturbance accommodating controller. We see that the frequency deviation for both machines becomes zero in a very short period of time.

This controller achieves an efficient response with substantially smaller frequency deviation. The designed controller is robust to external and neighboring disturbances like small changes in the scheduled generation of one machine or a small load added to the system as well [7].

7. Conclusions

The integration of a fuel cell into the power distribution system is achieved in a systematic way by applying disturbance accommodation control theory. The designed controller makes optimal constructive use of the fuel cell output to enhance the overall performance of the integrated system. The performance of the controller is assessed through simulation of a two-area power system. The main objective of this control scheme is to keep the power system stable when a fuel cell is connected. The controller achieves a fast response with substantially small frequency deviation while maintaining the energy balance between generation and consumption.

We observe that the overall system stability depends not only on the dynamics of the power system but also on the dynamics of the fuel cell. The dynamics of the fuel cell does not affect the system stability when it is offline, but it definitely affects the overall system stability when it is on.

The controller developed in this paper will be used to carry out a detailed analysis of the different penetration levels of the fuel cell and its effects on the power quality of the overall system. As the penetration level of the fuel cell increases, the power quality will deteriorate and necessary control action must be taken. According to existing laws, the supplied power must meet certain standard requirements regarding harmonics and power factor.

The developed controller will also be very useful for reliability analysis of the overall system. We also need to determine the fault tolerance of the integrated power system during large disturbances.

All these efforts will eventually lead to the development of a cost-effective, decentralized power system involving significant penetration of distributed energy resources like fuel cells.

Acknowledgements

This research was sponsored in part by US-DOE/EPSCoR, WV state implementation award.

References

[1] J.J. Grainger, W.D. Stevenson, Power System Analysis, McGraw-Hill, New York, January 1994.
[2] H. Saadat, Power System Analysis, McGraw-Hill, New York, August 1998.
[3] A. Feliachi, On load frequency control, INFOR 29 (4) (1991) 295–304.
[4] C.D. Johnson, Theory Of Disturbance-Accommodating Controllers, in: Advances in Theory and Applications of Control and Dynamic Systems, vol. 12, 1976, pp. 389–471.
[5] C.D. Johnson, Disturbance utilizing controllers for noisy measurements and disturbances, Int. J. Control 39 (5) (1984) 859–868.
[6] P. Kundur, Power System Stability and Control, McGraw-Hill, New York, January 1994.
[7] A. Paradkar, Integration of a PEM Fuel Cell into Distribution System in a Deregulated Environment: A LFC Problem, MS Thesis, Control Systems Engineering, West Virginia University Institute of Technology, West Virginia, 2002.
[8] Fuel Cell Hand Book, fifth ed., US Department of Energy, National Energy Technology Laboratory, October 2000.
[9] R.S. Gemmen, Analysis for the effect of inverter ripple current on FC operating condition, in: Proceedings of the ASME 2001 International Mechanical Engineering Congress and Exposition, New York, NY, November 2001, pp. 26–42.
[10] S. Yerramalla, A. Davari, A. Feliachi, T. Biswas, Modeling and simulation of the dynamic behavior of a polymer electrolyte membrane fuel cell, J. Power Sources 124 (1) (2003) 104–113.
[11] M. Ilic, J. Zaborszky, Dynamics and Control of Large Electric Power Systems, Wiley–Interscience, March 2000.